10.1098/rsta.2000.0655

THE ROYAL SOCIETY

Laboratory spectroscopy of H_3^+

By Benjamin J. McCall

Department of Chemistry and Department of Astronomy and Astrophysics, University of Chicago, Chicago, IL 60637, USA

The experimental determination of the low-lying rovibrational energy levels of H_3^+ using high-resolution, high-sensitivity infrared laser spectroscopy has confirmed this ion's equilateral triangle equilibrium geometry, provided direct information on its quantum mechanical characteristics, and enabled its extensive study in planetary ionospheres and in the interstellar medium.

Since the discovery of the $\nu_2 \leftarrow 0$ fundamental band, the laboratory spectroscopy of H_3^+ has been pushed to higher energies through the study of vibrational hot bands, overtones, forbidden bands and combination bands. We review the 20 years of laboratory spectroscopy of this important ion, discuss our recent work on the $\nu_1 + 2\nu_2^2 \leftarrow 0$ and $2\nu_1 + \nu_2 \leftarrow 0$ bands, and examine the prospects for the future of H_3^+ spectroscopy.

Keywords: infrared spectroscopy; molecular ions, H_3^+; plasma spectroscopy

1. Introduction

Ever since H_3^+ was first identified in the laboratory by Thomson (1911), it has played a central role in the study of laboratory plasmas. Indeed, it is by far the most abundant ion in pure hydrogen discharges, owing to its stability and its efficient production from hydrogen. H_3^+ is also important in astrophysical plasmas (which are dominated by hydrogen) such as planetary ionospheres and the interstellar medium, where it serves as the cornerstone of ion–molecule chemistry.

H_3^+ is also of fundamental theoretical interest, because it is the simplest polyatomic molecule (consisting of only three protons and two electrons) and also possesses a high symmetry (D_{3h}) because of its equilateral triangle equilibrium geometry. While theoretical calculations are essential in predicting and understanding the structure of molecules such as H_3^+, experiment (in particular high-resolution spectroscopy) ultimately provides the decisive test of theory, and also provides the information necessary for the refinement of the calculations.

The immediate product of laboratory spectroscopy of H_3^+ is the determination of accurate transition frequencies, which are important to both astronomers and theoreticians. These frequencies have enabled astronomers to detect H_3^+ in the interstellar medium and in the atmospheres of Jupiter, Saturn, and Uranus, and also to use H_3^+ as a remote probe for studying these astrophysical plasmas. For theoreticians, these H_3^+ transition frequencies have determined the molecular structure and constants, allowed the refinement of *ab initio* potential surfaces, and permitted a direct comparison with the results of variational calculations. Ultimately, a complete theoretical understanding of the observed spectra of H_3^+ (the simplest polyatomic) should lead to improved calculations for more complicated polyatomic molecules.

2. Laboratory production of H_3^+

From a chemical perspective, the production of H_3^+ is quite straightforward. All that is necessary is H_2 and a source of ionization. In the laboratory, the ionization is provided by electron impact in a plasma:

$$H_2 + e^- \rightarrow H_2^+ + 2e^- . \tag{2.1}$$

The production of H_3^+ then proceeds rapidly through the reaction

$$H_2^+ + H_2 \rightarrow H_3^+ + H, \tag{2.2}$$

which proceeds with the Langevin rate coefficient of 2×10^{-9} cm^3 s^{-1} (Bowers *et al.* 1969).

Experimentally, however, it is necessary to design a vessel to contain the plasma and optimize the conditions to produce the maximum amount of H_3^+. Two primary types of vessels have been used for the production of H_3^+: the hollow cathode cell (which exploits the negative glow region of the plasma); and the positive column cell (which exploits the positive column glow). Here I will focus on the positive column cell, which has been used most extensively for laser absorption spectroscopy of H_3^+.

A diagram of one of the discharge cells used to produce H_3^+ is shown in figure 1. The central bore of the cell (which contains the plasma) is *ca.* 1 m in length and 18 mm in diameter. The reagent gas is continuously flowed in through multiple inlets and pumped out through several outlets. This continuous flow of fresh reagent gas is essential when studying carbocations, but less important for H_3^+. To either end of the central bore is attached a fixture that contains both a Brewster window (to pass the laser radiation) and an electrode (which drives the plasma). Just outside of the central bore is a concentric volume, which contains the coolant (in this case liquid nitrogen). The outermost jacket is evacuated to provide thermal insulation for the liquid nitrogen.

The reagent gas used to produce H_3^+ is pure H_2 at a pressure of *ca.* 500–800 mTorr. In certain situations, it is preferable to add *ca.* 5–10 Torr of He as a buffer gas. Typically, a voltage of *ca.* 6 kV is applied across the electrodes, and a current density of *ca.* 60 mA cm^{-2} flows through the cell. Interestingly, these discharge conditions combined with a multiple-reflection cell lead to column densities (that is, concentration times absorption path length) of order 10^{14} cm^{-2}, comparable with those found in the interstellar medium!

Thermodynamically, the plasma discharge is a non-equilibrium system, but can be characterized to a first approximation by three different temperatures: the electron temperature (T_e), the vibrational temperature (T_v), and the rotational temperature (T_r). (The translational temperature is found to be closely coupled with the rotational temperature.) In the case of the positive column discharge, T_e is of the order of 10 000 K. T_v and T_r depend on the reagent gas used and the cooling method employed. For liquid-nitrogen-cooled cells, Bawendi *et al.* (1990) have spectroscopically measured $T_v \sim 600$ K and $T_r \sim 300$ K for pure-H_2 discharges and $T_v \sim 1000$ K and $T_r \sim 400$ K for H_2/He discharges. For a water-cooled cell, Uy *et al.* (1994) have measured $T_r \sim 1000$ K for a H_2/He discharge.

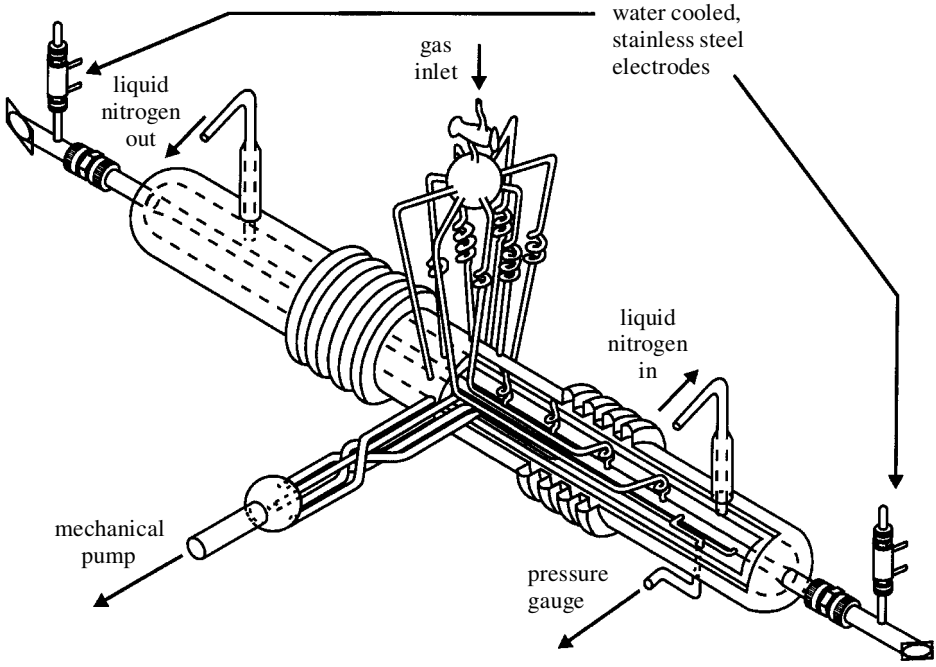

Figure 1. Liquid-nitrogen-cooled discharge cell used for producing H_3^+ (illustration by C. M. Lindsay).

3. Spectroscopy of H_3^+

(*a*) *Electronic spectroscopy*

For many molecules, electronic spectroscopy is a powerful probe of molecular structure both in the laboratory and in astronomical objects. However, this is not the case for H_3^+, which does not possess a stable electronic excited state. It is thought that H_3^+ has an excited triplet state (Friedrich & Alijah 2000) that lies above the dissociation energy to $H_2 + H^+$, but this would be difficult to probe spectroscopically.

(*b*) *Rotational spectroscopy*

Another important tool for the study of most molecules is rotational spectroscopy. This tool is particularly useful in detecting interstellar molecules because of the high sensitivity of radioastronomy.

The equilateral triangle geometry of H_3^+ suggests that this ion does not possess a permanent dipole moment, which is necessary for a rotational spectrum. However, centrifugal distortion caused by the rotation of the molecule can produce a small dipole moment, which leads to a weak 'forbidden' rotational spectrum (Watson 1971). The forbidden rotational spectrum of H_3^+ has been calculated by Pan & Oka (1986) to be several orders of magnitude weaker than typical allowed rotational spectra. It is worth noting that because of the small nuclear masses and large anharmonicity of H_3^+, even this weak spectrum is two to three orders of magnitude stronger than the forbidden rotational spectra of other molecules such as NH_3 and CH_4.

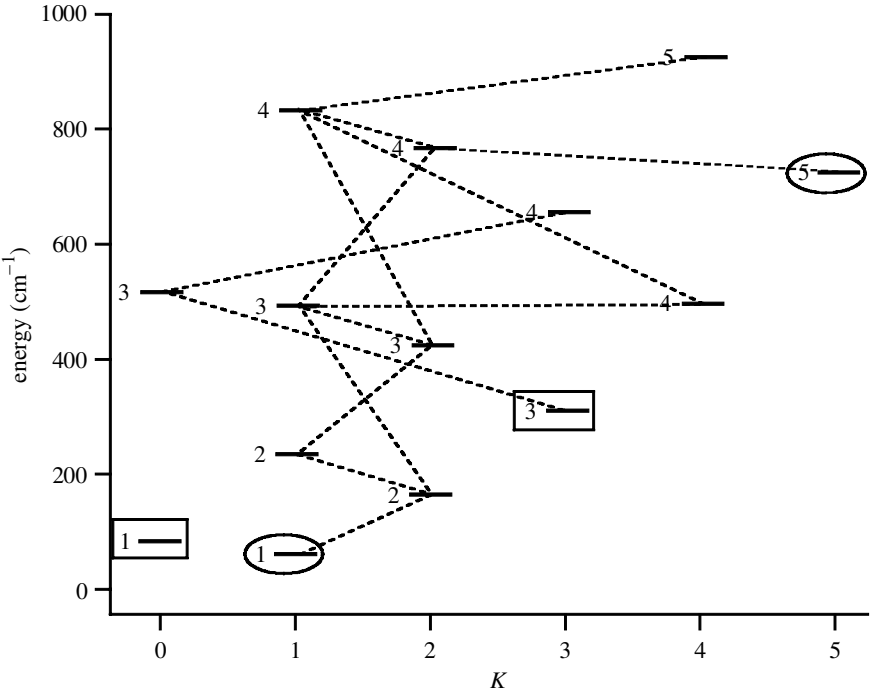

Figure 2. Energy-level diagram of the ground vibrational state of H_3^+. The numbers to the left of the levels are the values of J. The broken lines indicate the forbidden rotational transitions. The radiatively stable states are indicated by rectangles (ortho) and ovals (para).

These forbidden rotational transitions play an important role in the relaxation of H_3^+ in the interstellar medium, where their spontaneous emission times are shorter than the collision time-scale.

The rotational energy-level structure of the ground vibrational state of H_3^+ is shown in figure 2. The quantum numbers which describe the ground state are J, the angular momentum of the nuclear motion, and $K = |k|$, the magnitude of the projection of J onto the symmetry axis of the molecule. The structure is that of an oblate symmetric top, with the exception that the (J even, $K = 0$) levels are forbidden by the Pauli principle. One particular consequence of this is that the usual ground state (0,0) does not exist, leaving (1,1) as the lowest state.

Since H_3^+ consists of three protons (each with nuclear spin $I = \frac{1}{2}$), it possesses two spin modifications: ortho-H_3^+, in which all three spins are aligned and $I = \frac{3}{2}$; and para-H_3^+, in which one spin is antiparallel and $I = \frac{1}{2}$. Due to symmetry requirements on the total wave function, ortho-H_3^+ exists only with $K = 3n$ and para-H_3^+ exists only with $K = 3n \pm 1$, where n is an integer. The ortho and para spin modifications of H_3^+ are not connected by radiative transitions. The parity of the rotational levels is given by $(-1)^K$.

The selection rules for the forbidden rotational spectrum are $\Delta J = 0, \pm 1$ and $\Delta k = 3$. These transitions are indicated in figure 2 as dashed lines. It is interesting to note that the levels (1,0), (3,3) and (5,5) are not connected to any lower states by rotational transitions; thus, they are radiatively stable. The rotational spectrum of H_3^+ spans over two decades in frequency, from *ca.* 7 to 1000 cm^{-1}. At the low

temperatures of the interstellar medium, the strongest transition (in absorption or emission) would be (2,2)–(1,1) at 105.177 cm^{-1}.

(*c*) *Vibrational spectroscopy*

H_3^+ has two vibrational modes: the totally symmetric stretch ν_1 and the doubly degenerate stretch ν_2. The ν_2 mode possesses vibrational angular momentum, which is denoted by the quantum number ℓ_2. If v_2 is the number of quanta in the ν_2 mode, then $\ell_2 = v_2, v_2 - 2, \ldots, -v_2$. Because of an effect known as 'ℓ-resonance', rovibrational levels with different values of k and ℓ_2 but with the same value of $|k - \ell_2|$ are severely mixed. The result of this is that k and ℓ_2 are individually no longer good quantum numbers in vibrational states with $v_2 \neq 0$; instead, we define a new quantum number $g \equiv k - \ell_2$ that physically represents the part of the projection of J that is due to rotation. The connection with spin modification in $v_2 \neq 0$ states is through $G \equiv |g|$: ortho-H_3^+ must have $G = 3n$ and para-H_3^+ must have $G = 3n \pm 1$. Because $G = K$ in the vibrational ground state, it is convenient to use G rather than K in all states.

Theoretical calculations of the vibrational energy structure of H_3^+ are based on the potential energy surface, which describes the 'electronic energy' of the molecule as a function of the nuclear coordinates. Figure 3 shows a one-dimensional version of the potential energy surface of Röhse *et al.* (1994). This surface has been generated by forcing two of the H–H bonds to be of equal length, but allowing that length to vary for each value of θ (the angle between these two H–H bonds) in order to find the minimum energy for that value of θ. For small values of θ, the potential surface rises sharply, corresponding to the Coulomb repulsion between the two protons being brought close together. For $\theta \to \pi$, the potential surface rises but then flattens out; this is known as the 'barrier to linearity' because at $\theta = \pi$, H_3^+ becomes a linear molecule.

Also plotted in figure 3 are the theoretical rotationless ($J = 0$) vibrational states of H_3^+, from the calculations of J. K. G. Watson (1999, personal communication). Note that the ground state ($v_1 = v_2 = 0$) lies 4364 cm^{-1} above the bottom of the potential; this is the zero point vibrational energy of H_3^+. States with $v_2 > 1$ have multiple substates corresponding to the different values of $|l_2|$. For clarity, the states have been separated horizontally based on their values of v_1.

Five types of vibrational transitions can be studied. The *fundamental* band $\nu_2 \leftarrow 0$ is by far the strongest band, and was the first to be studied in the laboratory (Oka 1980). *Overtone* bands are transitions of the type $n\nu_2 \leftarrow 0$, representing multiple excitations of the ν_2 mode. *Hot* bands are transitions starting from vibrationally excited states, such as $2\nu_2 \leftarrow \nu_2$ and $\nu_1 + \nu_2 \leftarrow \nu_1$. *Forbidden* bands are transitions which involve only excitations of the infrared-inactive ν_1 mode, such as $\nu_1 \leftarrow 0$ and $\nu_1 + \nu_2 \leftarrow \nu_2$. Finally, *combination* bands are transitions from the ground state to states which are excited in both ν_1 and ν_2, such as $\nu_1 + 2\nu_2 \leftarrow 0$ and $2\nu_1 + \nu_2 \leftarrow 0$.

Figure 4 shows the band centres and intensities of the strongest vibrational bands, at an assumed temperature of 600 K. The values of the band origins as well as their intensities are calculated from the predictions of Dinelli *et al.* (1992). Hot bands are labelled with arrows, and the superscripts above ν_2 are the values of $|\ell_2|$ ($|\ell_2| = 1$ is omitted in the ν_2 state for brevity). Also shown, at the top of the figure, are the different tunable radiation sources available for H_3^+ spectroscopy, and their

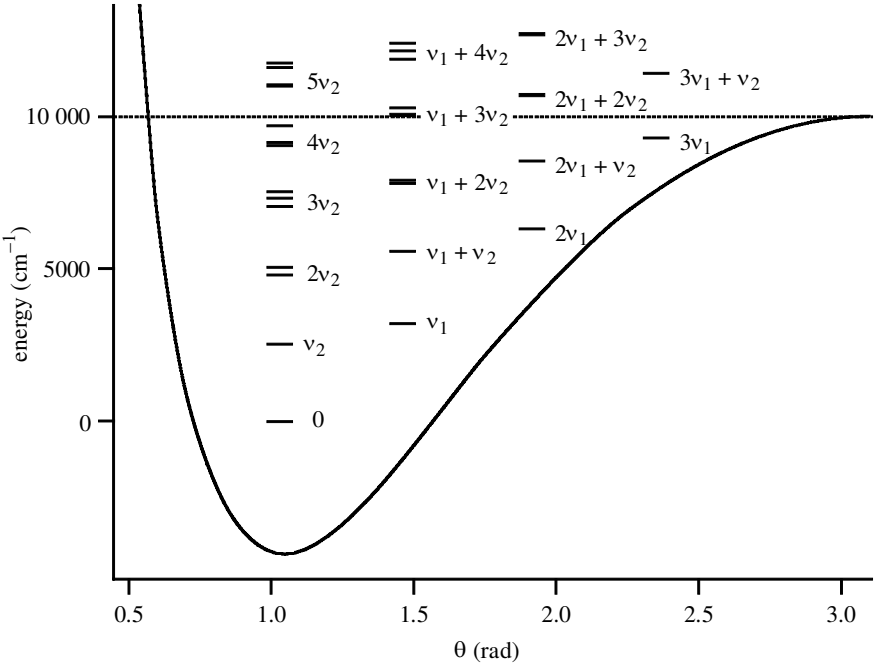

Figure 3. A one-dimensional representation of the potential surface of H_3^+, where two H–H bond lengths are required to be equal, and the angle between them (θ) is varied. Also shown are the calculated vibrational energy levels ($J = 0$) from the calculations of J. K. G. Watson and the barrier to linearity (dotted line).

approximate power (on the right axis). The bars at the bottom of the diagram show the spectral ranges which have been continuously scanned with laser spectroscopy (tall light-grey bars) and Fourier transform infrared (FTIR) spectroscopy (medium dark-grey bars). Also indicated (short bar) is the region where work is in progress using laser spectroscopy.

4. The $\nu_2 \leftarrow 0$ fundamental band

The ν_2 fundamental band is by far the strongest spectral signature of H_3^+. Using a cell such as the one shown in figure 1, and a multiple-reflection system that allows eight passes through the cell, the strongest lines of the fundamental are of the order of 5% deep. The strongest lines in this band can therefore be observed using direct absorption spectroscopy (both in the laboratory and in the interstellar medium). Consequently, this was the first band of H_3^+ to be observed and has been studied in more detail than any other band.

The $\nu_2 \leftarrow 0$ band of H_3^+ was first observed 20 years ago by Oka (1980). Because H_3^+ is such a light molecule, it has very large rotational constants ($B \sim 44\,\mathrm{cm}^{-1}$), and its spectrum is spread out over a wide frequency range. After a search of over two years, Oka (1980) scanned 500 cm^{-1} and was rewarded with only 15 lines! Oka knew approximately what frequency range to scan, thanks to the *ab initio* calculations of Carney & Porter (1976). While the search for this spectrum was lengthy, the assignment was completed by Watson overnight.

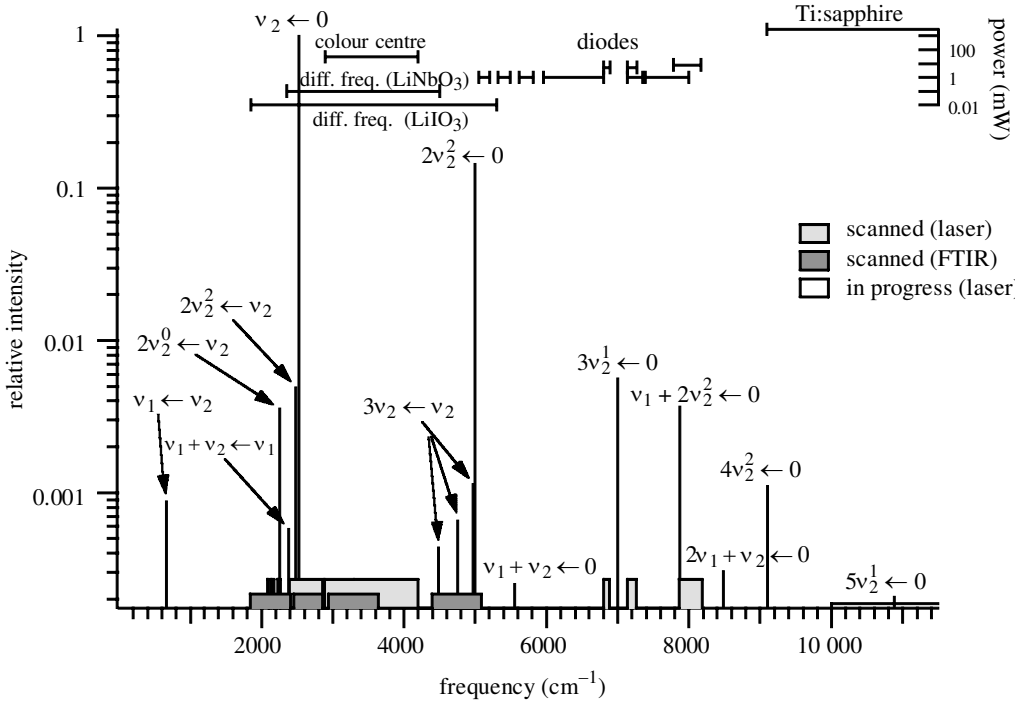

Figure 4. Vibrational band centres of H_3^+ and their relative intensities (note logarithmic scale) in absorption at 600 K. See text for explanation.

Within a year, the number of observed transitions had been doubled to 30 (Oka 1981). In another three years the number had risen to 46 (Watson *et al.* 1984), and the next three years saw a rise to 113 (Majewski *et al.* 1987) using FTIR emission spectroscopy. By this time, transitions starting from J as high as 9 had been observed. In 1990, Nakanaga *et al.* (1990) reported the first FTIR absorption spectrum of H_3^+. Uy *et al.* (1994) extended the spectroscopy of the fundamental band up to $J = 15$ using a water-cooled discharge, and found 38 new lines. Majewski *et al.* (1994) found an additional 55 lines of the fundamental band using FTIR emission spectroscopy. Recent work has been performed by Joo *et al.* (2000), who found the lowest frequency line to date at 1546.901 cm^{-1}, and by Lindsay *et al.* (2000*a*), who observed new lines in the region 3000–3600 cm^{-1}. Also of note is the recent work of McKellar & Watson (1998), who presented the first wide-band spectrum of the fundamental band of H_3^+, using FTIR absorption spectroscopy.

The observed spectrum of the $\nu_2 \leftarrow 0$ fundamental of H_3^+ is shown in figure 5. Since laboratory intensities are not as reliable (for technical reasons) as theoretical intensities, the intensities in the figure have been computed based on a temperature of 400 K from the theoretical calculations of Watson (1992, personal communication).

This observed spectrum immediately yields both qualitative and quantitative information about the structure of H_3^+. Qualitatively, the lack of an $R(0)$ line shows that this molecule possesses three equivalent fermions with spin $\frac{1}{2}$ (as discussed above, the (0,0) state is forbidden by the Pauli principle), and therefore has an equilateral triangle equilibrium structure. Furthermore, the intensity variations represent the 2:1 statistical weights of ortho:para H_3^+. The spacing between the sub-branches

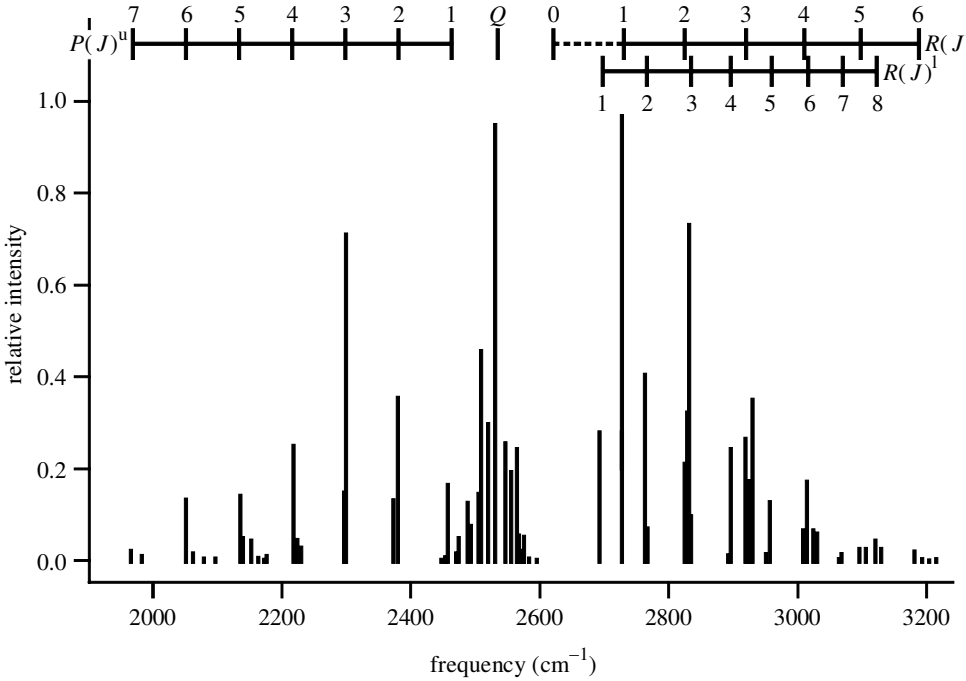

Figure 5. The observed spectrum of the ν_2 fundamental of H_3^+. The intensities are theoretical, assuming a temperature of 400 K. The branches and sub-branches are noted along the top; note in particular the absence of an $R(0)$ line, proof that all three protons are equivalent.

(most easily seen in the P-branch) illustrates the large rotational constants. Quantitatively, the frequencies of the observed transitions can be fitted to those predicted by an effective Hamiltonian in order to compute not only the rotational constants, but also higher-order terms in the perturbation treatment. The observation of this band also fixes the energy of the ν_2 level (2521 cm^{-1}).

The $\nu_2 \leftarrow 0$ fundamental band has proven to be an exceptionally useful probe of H_3^+, both in the laboratory and in space. In the laboratory, it has been used as a spectroscopic probe in studying the H_3^+ electron recombination rate (Amano 1988), the spin conversion of H_3^+ in chemical reactions (Uy *et al.* 1997), and the rate of ambipolar diffusion in plasmas (Lindsay *et al.* 2000*b*). Astronomically, it has served as a remote probe of the ionospheres of the giant planets (Connerney, this issue; Miller, this issue), and has also enabled the direct confirmation of the ion–molecule scheme of interstellar chemistry (Geballe, this issue; Herbst, this issue).

5. A digression on notation

The notation used for labelling H_3^+ transitions deserves some explanation. While different notations have been used to describe H_3^+ transitions, there has not yet been one consistent notation that can be used for all types of transitions (fundamental, hot bands, etc.). Here, we introduce a new standard, which is more flexible than those previously used and can be used to label all of the lines likely to observed astronomically, as well as the vast majority of lines observed in the laboratory.

The limitations of this notation are that one must specify the vibrational band including $|\ell_2|$ (e.g. $\nu_1 + 2\nu_2^2 \leftarrow 0$) and that it assumes that G is an approximately good quantum number. In cases where the quantum numbers v_1, v_2, $|\ell_2|$ and G become so badly mixed that it is not possible to identify the dominant contribution to the mixing, this notation will fail. One must then resort to a full description of the rigorous quantum numbers (see § 10 and table 1). Fortunately, such badly mixed cases correspond to weak transitions, so these problems should not concern astronomers or laboratory spectroscopists studying relatively strong lines.

The new preferred notation for H_3^+ rovibrational transitions is:

$$^{[\mathrm{n}|\mathrm{t}]}\{P \mid Q \mid R\}(J,G)^{[\mathrm{u}|\mathrm{l}]}_{[\mathrm{u}|\mathrm{l}]}. \tag{5.1}$$

As is usual in spectroscopy, $\{P \mid Q \mid R\}$ represents $\Delta J = \{-1 \mid 0 \mid +1\}$, and (J, G) are the values of these quantum numbers in the lower state (G is preferred to K because the latter is not a good quantum number when $\ell_2 \neq 0$). The [u | l] is used to discriminate between the two levels of an ℓ-resonance pair (states with the same $G = |k - \ell_2|$ but different k and ℓ_2). If the transition originates from such a pair in the lower state, a subscript 'u' or 'l' is used to represent the upper or lower energy member of the pair. Similarly, if the transition ends in such a pair in the upper state, a superscript 'u' or 'l' is used. The labels + and − were previously used for this purpose, but these were often confused with parity. Finally, the superscripted n or t before the $\{P \mid Q \mid R\}$ is used for transitions (such as the first overtone) where $\Delta g = \mp 3$. For $\Delta g = 0$ transitions, neither n nor t is used.

6. The hot bands: $2\nu_2 \leftarrow \nu_2$ and $\nu_1 + \nu_2 \leftarrow \nu_1$

As mentioned above, hot bands are transitions starting from vibrationally excited states. At a temperature of 600 K (see figure 4), the hot bands are a few hundred times weaker than the fundamental. However, the addition of helium to a hydrogen discharge has been found to increase the vibrational temperature T_v to *ca.* 1000 K. At these temperatures, the hot bands are observed to be only about 50 times weaker than the fundamental. Using a helium-dominated liquid-nitrogen-cooled discharge, Bawendi *et al.* (1990) were able to observe 72 lines of the $2\nu_2^2 \leftarrow \nu_2$ band, 14 lines of the $2\nu_2^0 \leftarrow \nu_2$ band, and 21 lines of the $\nu_1 + \nu_2 \leftarrow \nu_1$ band.

While the $\nu_2 \leftarrow 0$ fundamental band could be understood using a perturbation approach, this was not the case for the hot bands. Because of the small nuclear masses and the highly anharmonic potential of H_3^+, different rovibrational states are badly mixed and the traditional perturbation approach does not work well. In assigning the hot bands, the variational calculations developed by Sutcliffe (1983) and applied to H_3^+ by Miller & Tennyson (1988, 1989) were essential. As Bawendi *et al.* (1990) stated,

> probably the best strategy for this molecule is to provide the *ab initio* theorists with our experimentally determined energy levels so that they can further adjust... their potentials and accurately predict new rovibrational transitions.

The hot band transitions have also found their place in astronomy. The temperature of Jupiter's ionosphere (*ca.* 1000 K) is sufficiently high that the emission of

hot bands is observable. The simultaneous observation of both fundamental and hot band transitions provides an accurate 'thermometer' of this hot astronomical plasma. During the collision of comet Shoemaker–Levy 9 with Jupiter in 1994, Jupiter's ionosphere was significantly heated, and a strong hot band transition was observed alongside transitions of the fundamental (Dinelli *et al.* 1997).

7. The overtone bands: $2\nu_2 \leftarrow 0$ and $3\nu_2 \leftarrow 0$

In ordinary molecules, the first overtone band ($2\nu_2 \leftarrow 0$) is orders of magnitude weaker than the fundamental. In the case of H_3^+, because of the small masses and large anharmonicity in the potential surface, the first overtone is only about a factor of 7 times weaker.

In hindsight, the first overtone band was initially detected in emission at the time of the early observations of the ν_2 band (Majewski *et al.* 1987). However, as this spectrum also contained many emission lines of H_2 and neutral H_3, an assignment of the H_3^+ lines was not possible. In 1987–1988, a series of unidentified emission lines from the ionosphere of Jupiter was observed (Trafton *et al.* 1989; Drossart *et al.* 1989). After a month's work, Watson was able to assign these lines (and from there, many of the laboratory lines) to the $2\nu_2$ band of H_3^+. His assignment was aided by the laboratory observations of the $2\nu_2^2 \leftarrow \nu_2$ hot band (Bawendi *et al.* 1990), and indirectly by the variational calculations of Miller & Tennyson (1989) used to assign the hot band spectrum. In the end, 47 transitions of the first overtone band were assigned (Majewski *et al.* 1989). Subsequently, 27 of these lines (as well as seven new lines) were observed in absorption using a difference frequency laser spectrometer (Xu *et al.* 1990), yielding more accurate transition frequencies.

The second overtone band of H_3^+ is approximately 200 times weaker than the fundamental band. Using tunable diode lasers, 15 transitions of this band have been observed (Lee *et al.* 1991; Ventrudo *et al.* 1994). These transitions were assigned based on the variational calculations of Miller & Tennyson (1988, 1989), which were accurate to within a few cm^{-1}.

8. Absolute energy levels

The fundamental band and the hot bands obey the selection rule $\Delta G = 0$ because they involve a single excitation of the ν_2 mode. Using these transitions, it is therefore only possible to experimentally determine the relative energies of different rovibrational states with the same value of G. However, with the observation of the first overtone (which obeys the selection rule $\Delta G = \pm 3$), it was possible to fix the separations between levels with different G values for all ortho-H_3^+ energy levels and for all para-H_3^+ levels. Although ortho- and para-H_3^+ are not radiatively coupled, their relative energies can be fixed by fitting the energies of the ground state (J, K) levels to the symmetric rotor energy formula. In this way, experiments now yield absolute H_3^+ energy levels completely independent of theoretical predictions.

9. The forbidden bands: $\nu_1 \leftarrow 0$ and $\nu_1 + \nu_2 \leftarrow \nu_2$

The transition $\nu_1 \leftarrow 0$ is forbidden in the sense that it involves only excitation of the infrared-inactive ν_1 mode. Such a transition is especially forbidden not only because

Table 1. *Observed transitions of the* $\nu_1 + 2\nu_2^2$ *and* $2\nu_1 + \nu_2^1$ *bands of* H_3^+*, along with the quantum numbers and expectation values of the upper and lower states from the calculations of J. K. G. Watson*

(Single prime denotes the upper state of the transition, double prime denotes the lower state.)

symbol	observed	calculated	J'	$\langle G' \rangle$	$\pm'$	o/p′	n'	$\langle v_1' \rangle$	$\langle v_2' \rangle$	$\langle l_2' \rangle$	J''	k''
${}^tQ(3,0)$	7785.233	7785.2642	3	3.0	−	o	12	1.0	2.0	−2.0	3	0
${}^tQ(1,0)$	7785.701	7785.3404	1	3.0	−	o	5	1.0	2.0	−2.0	1	0
${}^tR(3,3)$	7789.878	7790.0248	4	5.9	+	o	9	1.0	2.0	−2.0	3	3
${}^nP(1,1)$	7805.893	7805.8506	0	2.0	+	p	5	1.0	2.0	2.0	1	1
${}^nP(2,2)$	7820.239	7819.9804	1	1.0	−	p	12	1.0	2.0	2.0	2	2
${}^tR(2,2)$	7822.375	7822.2495	3	5.0	−	p	18	1.0	2.0	−2.0	2	2
${}^nP(3,3)$	7826.739	7826.6791	2	0.0	+	o	6	1.0	2.0	2.0	3	3
${}^nP(4,4)^{\mathrm{l}}$	7833.249	7833.4442	3	1.1	−	p	21	1.0	2.0	1.8	4	4
${}^tR(1,1)$	7850.959	7850.6766	2	4.0	+	p	15	1.0	2.0	−2.0	1	1
${}^tR(4,3)$	7880.921	7881.4428	5	5.9	+	o	13	1.0	2.0	−2.0	4	3
${}^nQ(1,1)$	7894.711	7894.3784	1	2.0	+	p	5	1.0	2.0	2.0	1	1
${}^nQ(2,1)$	7898.371	7898.1873	2	2.0	+	p	17	1.0	2.0	2.0	2	1
${}^nQ(3,1)$	7905.717	7905.8910	3	2.0	+	p	17	1.0	2.0	1.9	3	1
${}^tR(3,2)$	7912.047	7912.1958	4	4.9	−	p	18	1.0	2.0	−2.0	3	2
${}^tR(2,1)$	7939.619	7939.4988	3	4.0	+	p	15	1.0	2.0	−2.0	2	1
${}^tR(1,0)$	7970.413	7970.1244	2	3.0	−	o	5	1.0	2.0	−2.0	1	0
${}^nQ(2,2)$	7998.890	7998.7540	2	1.0	−	p	12	1.0	2.0	2.0	2	2
${}^tR(4,2)$	8005.582	8006.4406	5	4.8	−	p	30	1.0	2.0	−1.9	4	2
${}^nQ(3,2)^{\mathrm{u}}$	8007.410	8007.6278	3	1.0	−	p	22	1.0	2.0	1.9	3	2
${}^nQ(4,2)^{\mathrm{u}}$	8022.012	8022.6927	4	1.0	−	p	22	1.0	2.0	1.7	4	2
${}^tR(3,1)$	8027.840	8028.3370	4	3.5	+	p	26	1.0	2.0	−1.8	3	1
${}^nR(3,1)^{\mathrm{l}}$	8037.673	8038.1911	4	2.4	+	p	27	0.9	2.1	1.7	3	1
$P(6,6)$	8053.382	8054.8101	5	5.5	−	o	17	1.8	1.2	−1.2	6	6
${}^nR(1,1)$	8071.617	8071.4139	2	2.0	+	p	17	1.0	2.0	2.0	1	1
${}^nQ(4,3)$	8089.406	8090.2817	4	0.1	+	o	11	1.0	2.0	2.0	4	3
${}^nQ(3,3)$	8110.069	8110.2024	3	0.0	+	o	11	1.0	2.0	1.8	3	3
$P(5,5)$	8123.128	8123.9852	4	4.8	+	p	30	1.9	1.1	−1.1	5	5
${}^tR(4,1)$	8128.280	8129.3311	5	3.4	+	p	27	0.9	2.1	−1.8	4	1
${}^tR(3,0)$	8162.653	8163.3190	4	2.9	−	o	12	1.0	2.0	−1.9	3	0
${}^nR(2,1)$	8163.129	8163.2943	3	2.0	+	p	17	1.0	2.0	1.9	2	1

this $A_1 \leftarrow A_1$ transition is vibrationally forbidden, but also because there is no Coriolis coupling between the ν_1 and ν_2 states. The first mixing term is due to the effect of a vibration–rotation interaction known as 'Birss resonance' (Majewski *et al.* 1987). This mixing term is $\kappa^4 \sim 10^{-4}$ smaller than the vibrational energy and the mixing is only effective (and, hence, the transitions only observable) when there is an 'accidental' degeneracy between a state in ν_1 and a state in ν_2 with the same value of J and with G different by 3. Such a degeneracy only occurs for fairly high J, where the variation in rotational energy with G can compensate for the difference in vibrational energy (656.9 cm^{-1}). Nine such weak transitions into states with $J = 5$–7 were observed by Xu *et al.* (1992). This work determined the energy of the ν_1 level

to be 3178 cm^{-1}, in agreement with the value derived from the Rydberg spectrum of H_3 (Ketterle *et al.* 1989).

The $\nu_1 + \nu_2 \leftarrow \nu_2$ band is less forbidden, because the anharmonicity of the H_3^+ potential energy surface suffices to mix the $\nu_1 + \nu_2$ state with other vibrational states such as $2\nu_2^2$ and $3\nu_2^1$. The resulting mixing with the upper states of allowed hot band transitions leads to intensity borrowing, which makes the $\nu_1 + \nu_2 \leftarrow \nu_2$ band observable, though still weak. Nevertheless, Xu *et al.* (1992) were able to observe 21 lines in this band.

10. Combination bands: $\nu_1 + 2\nu_2 \leftarrow 0$ and $2\nu_1 + \nu_2 \leftarrow 0$

The $\nu_1 + 2\nu_2$ and $2\nu_1 + \nu_2$ vibrational states are among the highest energy states below the barrier to linearity (see figure 3). The combination bands from the vibrational ground state into these states are weaker than any allowed bands previously observed (see figure 4). The spectroscopy of these combination bands is very exciting because it represents the best test yet of theoretical calculations of H_3^+.

A tunable external cavity diode laser spectrometer was assembled specifically for the study of these bands. This diode laser has a nominal tuning range of 7633–8183 cm^{-1}, but due to degradation of the anti-reflection coating on the front facet of the diode, it only has a useful tuning range of *ca.* 7780–8168 cm^{-1}. The effect of this degradation is most severe on the low-frequency side, such that continuous scanning is only possible between *ca.* 7850 and *ca.* 8168 cm^{-1}.

Using the liquid-nitrogen-cooled discharge in figure 1, we continuously scanned both a pure hydrogen discharge ($P_{H_2} \sim 500$ mTorr) and a helium-dominated discharge ($P_{He} \sim 10$ Torr, $P_{H_2} \sim 500$ mTorr) from 7850 to 8168 cm^{-1}. Additionally, narrow (2 cm^{-1}) scans were made at the frequencies in the range of 7785–7850 cm^{-1} where H_3^+ lines were expected from theoretical calculations. In the course of this scanning we observed 30 transitions of H_3^+ and over 200 transitions between Rydberg states of H_2. The latter were easily discriminated against because of their greatly reduced intensity when helium was added to the discharge. A stick diagram of the observed H_3^+ spectrum is shown in figure 6, where the stronger lines have been labelled in accordance with the convention of expression (5.1). The intensities in figure 6, and the majority of our assignments, are taken directly from the calculations of J. K. G. Watson (1996, personal communication). Of the 30 H_3^+ transitions, two belong to the high-J portion of the P-branch of the $2\nu_1 + \nu_2 \leftarrow 0$ band, while the rest all belong to the $\nu_1 + 2\nu_2^2 \leftarrow 0$ band.

Table 1 includes the observed transitions and the calculated frequencies from Watson (1996, personal communication). In most cases, the observed frequencies are accurate to *ca.* 0.01 cm^{-1}. Also listed, from Watson's calculations, are the quantum numbers of the upper (primed) and lower (double-primed) states of each transition. Note that at these high energies, the quantities G and $|\ell_2|$ are no longer good quantum numbers; as a result, the expectation values of these quantities are given. This is also true, though to a lesser extent, of the quantities v_1 and v_2 (the number of quanta in each vibrational mode).

At these high energies, the only rigorous quantum numbers are J (the angular momentum of nuclear motion), the spin modification (ortho or para, listed as o/p in the table), and the parity ($\pm$). The quantity n in the table is not a quantum number, but simply a label giving the energy ordering of the states with the same $(J, \pm, \mathrm{o/p})$.

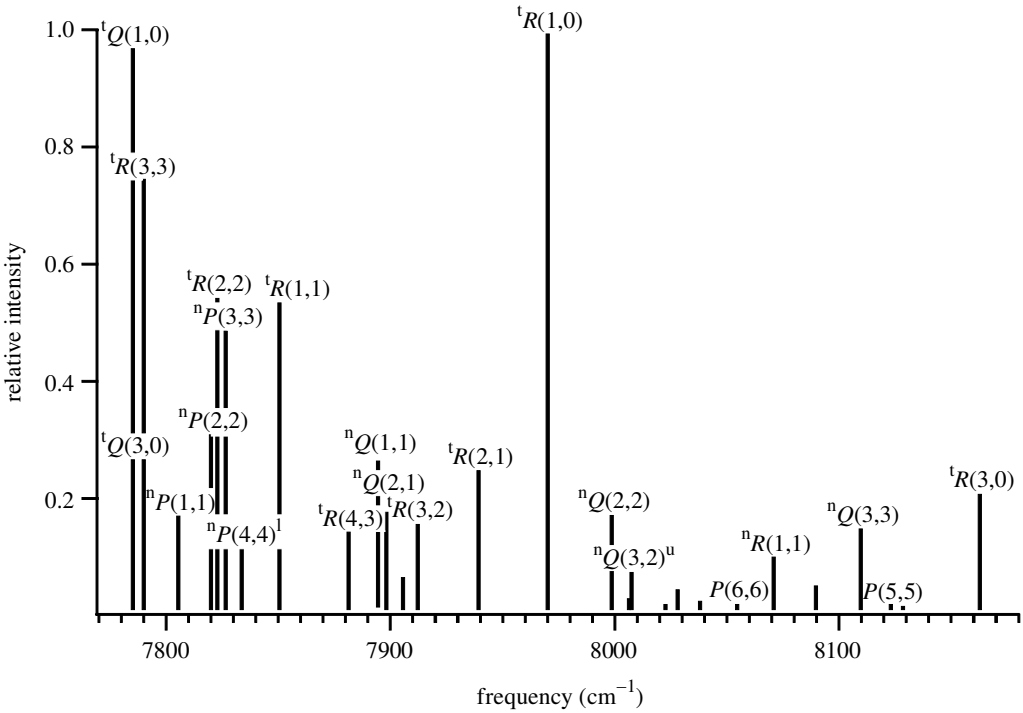

Figure 6. The observed spectrum of the $\nu_1 + 2\nu_2^2$ band of H_3^+, recently obtained using a tunable diode laser. The stronger lines are labelled as described in equation (5.1). The two weakest labelled lines belong to the $2\nu_1 + \nu_2^1$ band.

The failure of the traditional quantum numbers of H_3^+ is illustrated in figure 7, which shows the energy-level structure of the $\nu_1 + 2\nu_2^2$ vibrational state. The horizontal axis is the expectation value of G, and it is easily seen that the levels do not lie along vertical lines. Below each level the expectation value of ℓ_2 is listed, which should be ± 2, but is, in most cases, non-integral due to mixing.

The $\nu_1 + 2\nu_2^2 \leftarrow 0$ band is particularly amenable to astronomical observation, as it lies in a transparent spectral region of the atmosphere known as the J-band. While detection of this band in absorption in the interstellar medium is probably not feasible (since it is about 300 times weaker than the fundamental band), it may serve as a particularly useful probe of the emission from hot astronomical plasmas. At a vibrational temperature of 1000 K, this band is 25 000 times weaker than the fundamental, but by 1500 K this deficit is only 1700, at 2000 K it is down to only a factor of 450. Given the strong emission that has been observed from Jupiter's ionosphere, it is hoped that this band may serve as a thermometer for this type of environment.

11. Future prospects

In many ways, we have reached a milestone in the laboratory spectroscopy of H_3^+. With the exceptions of $2\nu_1$, $3\nu_1$, and $4\nu_2$, every vibrational state below the barrier to linearity has been studied in the laboratory. While the spectroscopy of these states

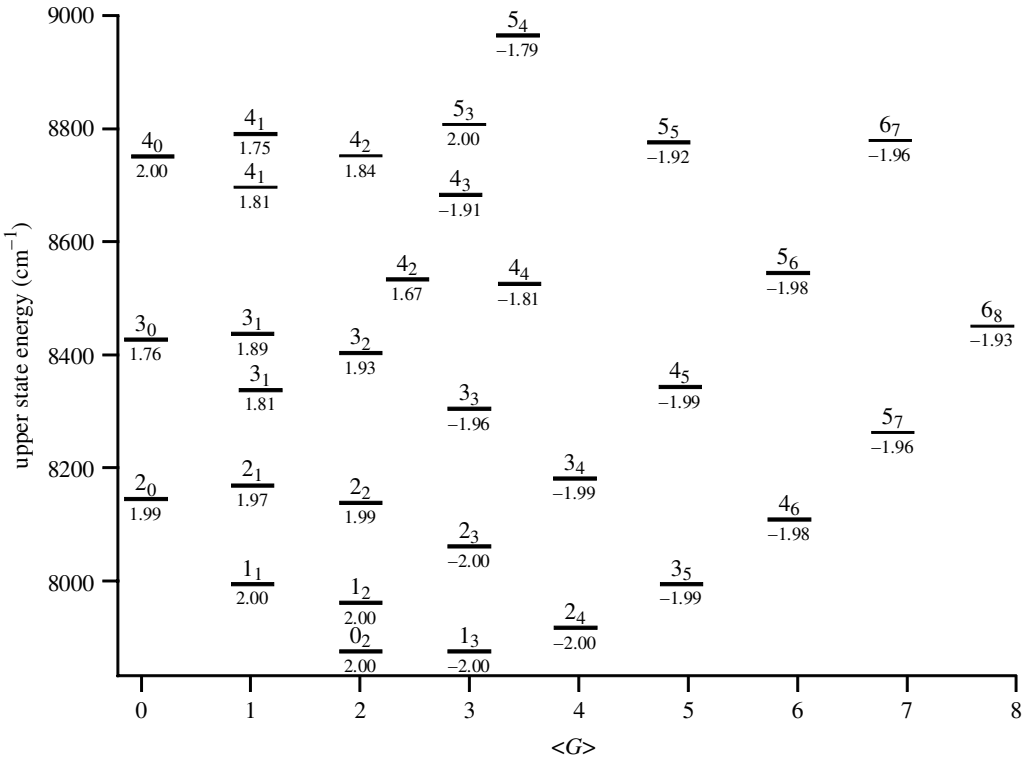

Figure 7. Energy-level diagram of the $\nu_1 + 2\nu_2^2$ vibrational state of H_3^+. The numbers above the levels are J_{G^*}, where G^* is the unmixed value of G. The numbers below the levels are the expectation value of $|\ell_2|$. Observed levels are indicated with heavy lines.

(and all of their $|\ell_2|$ substates) is by no means complete, we have established most of the band origins and filled in the rotational structure of many of the bands. State-of-the-art variational calculations based on spectroscopically adjusted potentials (e.g. J. K. G. Watson 1996, personal communication) now yield amazingly accurate predictions of both transition frequencies and intensities.

We are now entering a new era as we begin to probe the theoretically challenging region near and above the barrier to linearity. With our titanium:sapphire laser, we are preparing to attack $5\nu_2^1$, and perhaps even higher vibrational states. While these high overtones are very weak, they are well within reach given our current sensitivity. We expect that the breakdown of the G, $|\ell_2|$, and even v_1 and v_2 quantum numbers, which is already evident in our combination band spectra, will become even worse as we move to higher energies. Eventually, the energy-level diagrams may no longer even qualitatively resemble the ones in figures 2 and 7, but may be completely chaotic.

At the same time, theoreticians are rising to the challenge of predicting these high-energy vibrational states. Watson (this issue) is incorporating hyperspherical coordinates, which promise to alleviate the problems associated with linearity. On another front, Cencek *et al.* (1998) and Polyansky & Tennyson (1999) are working to incorporate relativistic and non-adiabatic effects into the rovibrational calculations.

Starting from $4\nu_2 \leftarrow 0$ (*ca.* 9000 cm^{-1}), the titanium:sapphire and ring-dye lasers provide continuous spectral coverage and ample power (watts) out to *ca.* 20 000 cm^{-1}.

With the introduction of new noise-reduction (e.g. heterodyne detection) and signal-enhancement (e.g. cavity) techniques, we may be able to continue the spectroscopy of H_3^+ out to $10\nu_2$ or even farther.

I acknowledge the assistance of T. Oka, who introduced me to this most remarkable molecular ion and has offered his insight and encouragement. I also thank J. K. G. Watson for helpful conversations and for providing the results of his calculations before publication. Finally, I thank the Fannie and John Hertz Foundation for their financial support. This work was also supported by NSF grant PHYS-9722691 and NASA grant NAG5-4070.

References

Amano, T. 1988 Is the dissociative recombination of H_3^+ really slow? A new spectroscopic measurement of the rate constant. *Astrophys. J.* **329**, L121–L124.

Bawendi, M. G., Rehfuss, B. D. & Oka, T. 1990 Laboratory observation of hot bands of H_3^+. *J. Chem. Phys.* **93**, 6200–6209.

Bowers, M. T., Elleman, D. D. & King Jr, J. 1969 Analysis of the ion–molecule reactions in gaseous H_2, D_2, and HD by ion cyclotron resonance techniques. *J. Chem. Phys.* **50**, 4787–4804.

Carney, G. D. & Porter, R. N. 1976 H_3^+: *ab initio* calculation of the vibration spectrum. *J. Chem. Phys.* **65**, 3547–3565.

Cencek, W., Rychlewski, J., Jaquet, R. & Kutzelnigg, W. 1998 Sub-micro-Hartree accuracy potential energy surface for H_3^+ including adiabatic and relativistic effects. I. Calculation of the potential points. *J. Chem. Phys.* **108**, 2831–2836.

Dinelli, B. M., Miller, S. & Tennyson, J. 1992 Bands of H_3^+ up to $4\nu_2$: rovibrational transitions from first principles calculations. *J. Mol. Spectrosc.* **153**, 718–725.

Dinelli, B. M., Miller, S., Achilleos, N., Lam, H. A., Cahill, M., Tennyson, J., Jacod, M.-F., Oka, T., Hilico, J.-C. & Geballe, T. R. 1997 UKIRT observations of the impact and consequences of Comet Shoemaker–Levy 9 on Jupiter. *Icarus* **126**, 107–125.

Drossart, P. (and 11 others) 1989 Detection of H_3^+ on Jupiter. *Nature* **340**, 539–541.

Friedrich, O. & Alijah, A. 2000 Triplet H_3^+. Exhibit, this meeting.

Joo, S.-W., Kühnemann, F., Jagod, M.-F. & Oka, T. 2000 Diode laser spectroscopy of the high J $P(12,12)^{\mathrm{u}}$ transition of H_3^+. Exhibit, this meeting.

Ketterle, W., Messmer, H.-P. & Walther, H. 1989 The ν_1 vibration of H_3^+ and autoionizing Rydberg states of H_3. *Europhys. Lett.* **8**, 333–338.

Lee, S. S., Ventrudo, B. F., Cassidy, D. T., Oka, T., Miller, S. & Tennyson, J. 1991 Observation of the $3\nu_2 \leftarrow 0$ overtone band of H_3^+. *J. Mol. Spectrosc.* **145**, 222–224.

Lindsay, C. M., Rade, R. M. & Oka, T. 2000*a* Survey of H_3^+ transitions between 3000 cm^{-1} and 4200 cm^{-1}. Exhibit, this meeting.

Lindsay, C. M., White, E. T. & Oka, T. 2000*b* Measurement of the H_3^+ destruction rate due to ambipolar diffusion in an AC positive column discharge. *Chem. Phys. Lett.* (In the press.)

McKellar, A. R. W. & Watson, J. K. G. 1998 The infrared spectrum of H_3^+ revealed. *J. Mol. Spectrosc.* **191**, 215–217.

Majewski, W. A., Marshall, M. D., McKellar, A. R. W., Johns, J. W. C. & Watson, J. K. G. 1987 Higher rotational lines in the ν_2 fundamental of the H_3^+ molecular ion. *J. Mol. Spectrosc.* **122**, 341–355.

Majewski, W. A., Feldman, P. A., Watson, J. K. G., Miller, S. & Tennyson, J. 1989 Laboratory observation of the $2\nu_2$ band of the H_3^+ molecular ion. *Astrophys. J.* **347**, L51–L54.

Majewski, W. A., McKellar, A. R. W., Sadovskiĭ, D. & Watson, J. K. G. 1994 New observations and analysis of the infrared vibration–rotation spectrum of H_3^+. *Can. J. Phys.* **72**, 1016–1027.

Miller, S. & Tennyson, J. 1988 Overtone bands of H_3^+: first principle calculations. *J. Mol. Spectrosc.* **128**, 530–539.

Miller, S. & Tennyson, J. 1989 Hot band transition frequencies and line strengths in H_3^+: first principles calculations. *J. Mol. Spectrosc.* **136**, 223–240.

Nakanaga, T., Ito, F., Sugawara, K., Takeo, H. & Matsumura, C. 1990 Observation of infrared absorption spectra of molecular ions, H_3^+ and HN_2^+, by FTIR spectroscopy. *Chem. Phys. Lett.* **169**, 269–273.

Oka, T. 1980 Observation of the infrared spectrum of H_3^+. *Phys. Rev. Lett.* **45**, 531–534.

Oka, T. 1981 A search for interstellar H_3^+. *Phil. Trans. R. Soc. Lond.* A **303**, 543–549.

Pan, F.-S. & Oka, T. 1986 Calculated forbidden rotational spectra of H_3^+. *Astrophys. J.* **305**, 518–525.

Polyansky, O. L. & Tennyson, J. 1999 *Ab initio* calculation of the rotation–vibration energy levels of H_3^+ and its isotopomers to spectroscopic accuracy. *J. Chem. Phys.* **110**, 5056–5064.

Röhse, R., Kutzelnigg, W., Jaquet, R. & Klopper, W. 1994 Potential energy surface of the H_3^+ ground state in the neighborhood of the minimum with micro-Hartree accuracy and vibrational frequencies derived from it. *J. Chem. Phys.* **101**, 2231–2243.

Sutcliffe, B. T. 1983 A comment on a recent proposal for the calculation of vibrational energies in the general triatomic molecule. *Mol. Phys.* **48**, 561–566.

Thomson, J. J. 1911 Rays of positive electricity. *Phil. Mag.* **21**, 225–249.

Trafton, L., Lester, D. F. & Thompson, K. L. 1989 Unidentified emission lines in Jupiter's northern and southern 2 micron aurorae. *Astrophys. J.* **343**, L73–L76.

Uy, D., Gabrys, C. M., Jagod, M.-F. & Oka, T. 1994 Spectral lines and distribution of H_3^+ in high rotational levels. *J. Chem. Phys.* **100**, 6267–6274.

Uy, D., Cordonnier, M. & Oka, T. 1997 Observation of ortho–para H_3^+ selection rules in plasma chemistry. *Phys. Rev. Lett.* **78**, 3844–3847.

Ventrudo, B. F., Cassidy, D. T., Guo, Z. Y., Joo, S., Lee, S. S. & Oka, T. 1994 Near infrared $3\nu_2$ overtone band of H_3^+. *J. Chem. Phys.* **100**, 6263–6266.

Watson, J. K. G. 1971 Forbidden rotational spectra of polyatomic molecules. *J. Mol. Spectrosc.* **40**, 536–544.

Watson, J. K. G., Foster, S. C., McKellar, A. R. W., Bernath, P., Amano, T., Pan, F. S., Crofton, M. W., Altman, R. S. & Oka, T. 1984 The infrared spectrum of the ν_2 fundamental band of the H_3^+ molecular ion. *Can. J. Phys.* **62**, 1875–1885.

Xu, L.-W., Gabrys, C. & Oka, T. 1990 Observation of the $2\nu_2\,(\ell = 2) \leftarrow 0$ overtone band of H_3^+. *J. Chem. Phys.* **93**, 6210–6215.

Xu, L.-W., Rösslein, M., Gabrys, C. M. & Oka, T. 1992 Observation of infrared forbidden transitions of H_3^+. *J. Mol. Spectrosc.* **153**, 726–737.

Discussion

G. Duxbury (*Department of Physics and Applied Physics, University of Strathclyde, UK*). In his paper, McCall demonstrated the range of laser spectrometric techniques which have been used successfully to map the mid- and near-infrared spectra of H_3^+. It has also been suggested that the far-infrared transitions induced by vibration–rotation mixing may also be detectable. It is the purpose of this comment to show that a new class of lasers, quantum cascade (or QC) lasers, have the potential to fill in many of the holes in the currently available tuning range of tunable lasers, in particular at the long-wavelength end of the infrared spectrum.

Quantum cascade lasers were first demonstrated by Faist *et al.* (1994), and are based upon electrons making transitions between energy levels created by quantum confinement. This confinement is in quantum wells created in semiconductors which

are based on gallium arsenide. Since the wavelength depends upon the quantum well structure and not upon the band gap of the parent semiconductor, the wavelengths of QC lasers may be tailored to operate over most of the region from 3 to 17 μm. These sources have much higher output power levels of between 10 and 20 milliwatts (Faist *et al*. 1994; Normand *et al*. 1999). They are much more compact and with lower power consumption than ion or YAG laser pumped difference frequency or F-centre lasers. They have also been shown to be excellent spectroscopic sources, with sufficient sensitivity to detect the ^{13}C and D content of methane (Kosterev *et al*. 1999), and have been shown to be frequency stabilized with a kilohertz linewidth (Williams *et al*. 1999).

The performance that has already been demonstrated (see Kosterev *et al*. 1999; Williams *et al*. 1999) shows that these lasers have the potential to be used not only to study the longer-wavelength transitions of ions such as H_3^+, but also other ions such as H_3O^+ and H_2O^+, which are interesting in the ion–molecule reactions. Williams *et al*. (1999) have also pointed out that these lasers have the potential to be part of a highly sensitive infrared heterodyne spectrometer, such as those currently based on CO_2 lasers.

Additional references

Faist, J., Capasso, F., Sivco, D. L., Sirtori, C., Hutchinson, A. L. & Cho, A. Y. 1994 *Science* **264**, 553.

Kosterev, A. A., Curl, R. F., Tittel, F. K., Gmachl, C., Capasso, F., Sivco, D. L., Baillargeon, J. N., Hutchinson, A. L. & Cho, A. Y. 1999 *Optics Lett.* **24**, 1762.

Normand, E., Duxbury, G., Langford, N. J., Farmer, C. & Ironside, C. N. 1999 In *16th Colloquium on High Resolution Molecular Spectroscopy, Dijon, 6–10 September 1999*, poster 4.

Williams, R. M. (and 10 others) 1999 *Optics Lett.* **24**, 1844.